Published in final edited form as:
Neuroscience. 2006 July 21; 140(4): 1359–1368.

AFFERENT REGULATION OF OXIDATIVE STRESS IN THE CHICK COCHLEAR NUCLEUS

A. H. NICHOLAS and **R. L. HYSON***
Department of Psychology, Program in Neuroscience, Florida State University, Tallahassee, FL 32306-1270, USA

Abstract

The chick auditory brain stem has been a useful model system for examining the afferent-dependent signals that regulate postsynaptic neurons. Like other sensory systems, compromised afferent input results in rapid death and atrophy of postsynaptic neurons. The present paper explores the possible contributions of an oxidative stress pathway in determining neuronal fate following deafferentation. Levels of reactive oxygen species, lipid damage measured by 4-hydroxynonenal formation, and a compensatory reactive oxygen species-induced response regulated by glutathione s transferase M1 and the reactive oxygen species-sensitive transcriptional factor, nuclear respiratory factor 1 were examined. Unilateral cochlea removal surgery was performed on young posthatch chicks. Labeling in the cochlear nucleus, nucleus magnocellularis, on opposite sides of the same tissue sections were compared by densitometry. The results showed a dramatic increase in reactive oxygen species in the deafferented nucleus magnocellularis by 6 h following cochlea removal. This increase in reactive oxygen species was accompanied by lipid damage and a compensatory upregulation of both glutathione s transferase M1 and nuclear respiratory factor 1. Double-labeling revealed that glutathione s transferase M1 expression was highest in neurons that were likely to survive deafferentation, as assessed immunocytochemically with Y10b, a marker for ribosomal integrity. Together, these data suggest reactive oxygen species are generated and a compensatory detoxifying pathway is upregulated in the first few hours following deafferentation. This is consistent with the hypothesis that oxidative stress plays a role in determining whether a given neuron survives following deafferentation.

Keywords

reactive oxygen species; auditory system; nucleus magnocellularis; deafferentation; cell death; antioxidant

---

Oxidative stress is the production of reactive oxygen species (ROS) beyond the cell's antioxidant capacity. While potentially toxic, ROS are necessary for normal cellular activities and are kept in balance by an antioxidant system. If the equilibrium between antioxidants and ROS is perturbed in favor of the latter, critical proteins, lipids and nucleic acids, essential to cellular homeostasis are oxidized (Ohinata et al., 2000; Cheng et al., 2001; Kelada et al., 2003). Often, these altered products initiate cellular cascades that culminate in apoptosis or necrosis (Tjalkens et al., 1998; Cheng et al., 2001). Although the relationship between oxidative stress and cell death is well documented in neurodegenerative diseases, such as Alzheimer's, Huntington's, and muscular dystrophies (Andersen, 2004; Cui et al., 2004), its role in the cascades of events that determine survival following deafferentation remains a mystery.

*Corresponding author. Tel: +1-850-644-5824; fax: +1-850-644-7739. E-mail address: hyson@psy.fsu.edu (R. L. Hyson)..

The chick auditory brain stem has been a useful model for examining the factors that regulate the life and death of postsynaptic CNS neurons following deafferentation. Its relatively simple and bilaterally symmetrical organization allows for within-subject comparative analysis. In this system, the ipsilateral auditory nerve provides the sole source of excitatory input to the cochlear nucleus, nucleus magnocellularis (NM). Thus, unilateral cochlea removal results in complete loss of excitatory input to the ipsilateral NM but leaves the contralateral side unaffected, thereby allowing comparison of NM neurons on the intact side versus the deafferented side of the same brain.

The elimination of sensory experience by cochlea ablation produces several dramatic changes in NM neurons. A few days (2–3) following cochlea removal, approximately 20–30% of NM neurons die, while the remaining show a reduction in soma size (Born and Rubel, 1985). Approximately 6 h following deafferentation, protein synthesis assays show two diverging and distinct pathways in NM. One population of NM neurons shows a reduce level of protein synthesis while the other, approximately 20–30% of the neurons, shows complete cessation of protein synthesis (Steward and Rubel, 1985). Similar effects of deafferentation can also be observed using Y10b, an antibody that recognizes ribosomal RNA (Garden et al., 1994). Prior to dissociating into two populations, decreased protein synthesis and Y10b labeling across all NM neurons can be visualized as early as one hour following deafferentation (Hyson and Rubel, 1989; Garden et al., 1994; Hyson, 1995). These early changes occur across the entire population of deafferented cells, therefore the factors that determine whether a given NM neuron will follow the survival pathway or the death pathway are still unknown. It is possible that the balance between pro-survival and pro-death mechanisms approaches a threshold that leaves some cells incapable of recovery. The precise nature of these pro-survival and pro-death influences, however, is also uncertain.

One possibility is that the response to oxidative stress predicts the survivability of a given neuron. A few studies have reported changes that suggest a perturbation of ROS homeostasis in NM. First, intracellular calcium is elevated within an hour of deafferentation (Zirpel et al., 1995). Elevated intracellular calcium has been shown to cause mitochondrial dysfunction that increases levels of ROS (review, Brookes et al., 2004). Additionally, 6 h following deafferentation, the mitochondria dramatically proliferate (Hyde and Durham, 1994). This is accompanied by a transient increase in oxidative enzyme capacity (Durham and Rubel, 1985; Hyde and Durham, 1990). Given that the mitochondrion is the major source of ROS production, a robust increase could cause elevated levels of ROS. Increases in ROS, however, can be counterbalanced by compensatory increases in antioxidant mechanisms. Perhaps the balance between ROS production and these compensatory responses determine whether an NM neuron will survive or die following deafferentation.

Typically, ROS indiscriminately attack polyunsaturated fatty acids of membranes consequently disrupting cellular integrity. Lipid peroxidation can be determined by measuring 4-hydroxynonenal (4-HNE), an α,β -unsaturated aldehyde that is produced from the reaction of ROS with the n-6 polyunsaturated lipids in the cellular membrane. The elevation of intracellular 4-HNE has been shown to activate the jun N-terminal kinase (JNK) pathway (Forman et al., 2003) and to cause cell cycle arrest (Yang et al., 2003) and apoptosis (Awasthi et al., 2003). In contrast, other studies have shown that the normal formation of 4-HNE can initiate differentiation and proliferation (Cheng et al., 1999), and the rise in levels of 4-HNE leads to the synthesis of the antioxidant, glutathione (GSH) (Liu et al., 1998).

Glutathione-S-transferases (GSTs) are one group of antioxidant effectors that respond to a variety of stresses (review, Hayes et al., 2005). These enzymes are classified into five classes (alpha, mu, pi, theta and zeta) based upon protein sequence, substrate specificity, and immunological properties (Clark, 1989; Rouimi et al., 1996). GSTs protect cellular

macromolecules from electrophilic attack through the conjugation of GSH to oxidized molecules such as 4-HNE. There is an emerging body of literature documenting the integral roles of GSTs in cell survival and death. For instance, numerous laboratories have shown that elevated levels of GST are associated with resistance to apoptosis (Kodym et al., 1999; Cumming et al., 2001). Moreover, forced expression of glutathione-S-transferase M1 (GSTM1) blocked apoptosis signal-regulating kinase (ASK1) -dependent cell death in cultured cells (Cho et al., 2001). It has been suggested that the induction of GST is an early adaptive response to oxidative stress; a response that is conserved across various species (review, Hayes et al., 2005).

Changes in GST expression have been shown to be regulated by Nrf1, the ROS-sensitive transcription factor. The increase in levels of ROS causes the translocation of Nrf1 into the nucleus resulting in the upregulation of detoxifying genes (Kang et al., 2004). The relevance of Nrf1 in this pathway is underscored by a study that showed Nrf1 deficiency results in early embryonic lethality and severe oxidative stress (Leung et al., 2003). The aim of the present study is to determine whether deafferentation inflicts oxidative damage but induces a compensatory change in GSTM1 expression in NM neurons. Toward this end, changes in ROS, 4-HNE, GSTM1, and Nrf1 were examined in NM following deafferentation. The results from this study are consistent with the hypothesis that an oxidative signaling pathway plays a role in the control of cell death following deafferentation.

EXPERIMENTAL PROCEDURES

Subjects

All subjects were Ross×Ross chickens that were hatched and reared at Florida State University. The procedures used in these experiments were approved by the Animal Care and Use Committee at The Florida State University and conform to the guidelines set forth by the National Institutes of Health. All efforts were made to minimize the number of animals used and their potential suffering. Subjects were 7–10 days posthatch for the experiments using immunocytochemistry. This age was chosen because the auditory system is presumed to be relatively mature by this time and because the majority of previous studies on the time course of changes following cochlea removal have been performed at this age (Rubel et al., 1990). The studies examining change in ROS required that younger chicks be used in order to obtain adequate dye loading.

Cochlea removal

A unilateral cochlear ablation was performed under halothane anesthesia. The ear canal was enlarged with small scissors then the tympanic membrane was punctured with forceps. The columella was removed, and the basilar papilla was extracted through the oval window using forceps. Finally, the middle ear cavity was packed with gelfoam, and the incision was closed with surgical adhesive. After recovery from anesthesia, the animals were placed back in their housing unit and allowed to survive for varying periods of time. The purpose of this surgical procedure was to eliminate all afferent drive to the ipsilateral NM while leaving the innervations to the contralateral NM intact.

Changes in ROS

All subjects were one day old post-hatched Ross×Ross chickens. Following unilateral cochlea removal surgery, the animals were allowed to survive for 1 (n=4), 6–8 (n=7), or 12 h (n=3).

Brain slicing for ROS detection

Following the survival period, subjects were anesthetized with halothane and decapitated. The brainstem was rapidly dissected from the cranium and mounted onto a custom-built stage for slicing using a vibrating-blade microtome. Dissecting and slicing were done in an artificial cerebrospinal fluid (ACSF) bath. The ACSF contained (in mM) NaCl, 130; KCl, 3; $CaCl_2$, 2; $MgCl_2$, 2; $NaHCO_3$, 26; NaH_2PO_4, 1.25; D-glucose, 10 and was oxygenated using a 95% O_2, and 5% CO_2 gas mixture. Care was taken during the dissection to preserve the auditory nerve on both sides of the brainstem. The brainstem was affixed to the microtome stage using cyanoacrylate glue and a 30% gelatin compound was placed under the lateral edges of the brainstem to provide additional support. A 150-μm, bilaterally symmetrical, coronal slice was obtained containing NM and the auditory nerve on both sides.

Dye loading

Intracellular production of ROS was detected with the ROS-sensitive fluorescent dye, carboxyl-2,7-dichlorodihydrofluorescin diacetate (H_2DCFDA, Molecular Probes, Carlsbad, CA, USA). Slices were incubated for 30 min at 37 °C in 5 μM H_2DCFDA. The H_2DCFDA was dissolved in dimethyl sulfoxide (DMSO) prior to adding it to the ACSF. Following incubation, slices were fixed in 4% paraformaldehyde for 10 min, washed 3× for 10 min in phosphate-buffered saline (PBS) then immediately mounted on electrostatically-charged microscope slides, coverslipped with VectaShield mounting media (Vector Laboratories, Burlingame, CA, USA) and sealed with commercially available nail polish. To minimize quenching, this procedure was performed under restricted lighting conditions.

Data analysis

Levels of H_2DCFDA fluorescence were objectively analyzed using densitometry. The slice was viewed under a 10× objective and a digital image was captured using a Spot RT camera (Diagnostics Instruments, Sterling Heights, MI, USA) for data analysis using the NIH ImageJ software. Densitometric measurements compared fluorescence intensity on the cochlea removal side to fluorescence intensity on the opposite (intact) side of the same slice. The group effect was determined with a one-way ANOVA and individual within-group effects were analyzed by *t*-test using Microsoft Excel and SPSS.

Immunocytochemistry

Surgery and sectioning—A unilateral cochlea ablation was performed on subjects P7-10 under halothane anesthesia. Immunolabeling for 4-HNE was examined 1–3 (n=4), 6 (n=3), 12 (n=5), or 24 h (n=3) following cochlea removal, immunolabeling for GSTM1 was examined 1 (n=3), 6 (n=4), 12 (n=3), or 24 h (n=3) following cochlea removal and immunolabeling for Nrf1 was examined 6 h (n=3) following cochlea removal.

At the end of their survival period, chicks were anesthetized with pentobarbital and perfused with room temperature 0.1 M phosphate buffer saline followed by ice cold 4% paraformaldehyde. After perfusion, the brain stem was removed from the skull, postfixed in 4% paraformaldehyde for 5 h then cryoprotected in 30% sucrose in PBS overnight. The following day, brain stems were frozen and sectioned at 20 μm on a cryostat, and these sections were collected into 0.1 M PBS.

Immunolabeling—Sections were rinsed 3× with PBS for 10 min, then preincubated in 1% normal goat serum, 1% Triton, and 1% bovine serum albumin (BSA) for 30 min, and then incubated in either anti-4-HNE (1:500), anti-GSTM1 (1:800), or anti-Nrf1 (1: 4000) diluted in blocking serum overnight at 4 °C. Anti-4-HNE was obtained from Chemicon International (Temecula, CA, USA), anti-GSTM1 was obtained from Upstate Biotechnology (Lake Placid,

NY, USA), and anti-Nrf1 was obtained from Santa Cruz Biotechnology (Santa Cruz, CA, USA). On the following day, sections were washed 3×10 min with PBS, then incubated in 1:200 biotin-ylated goat anti-rabbit secondary antibody, 1% normal goat serum, 1% Triton X-100, and 1% BSA for an hour. Sections then underwent another round of washing with PBS for 10 min and were then incubated in an avidin–biotin complex (Vector Laboratories, Burlingame, CA, USA) for one hour. Finally, for visualization, sections were reacted using 0.5-mg/ml diaminobenzidine and 0.009% hydrogen peroxide in phosphate buffer solution for approximately 20 min. Following washing with phosphate buffer, the sections were mounted on electrostatically charged microscope slides and allowed to dry overnight. The following day, sections were dehydrated in ascending series of alcohol concentrations (70%, 95% and 100%), cleared with xylenes, and coverslipped with DPX mounting media. No labeling was observed in control studies where the primary antibody was omitted.

Fluorescence double-labeling with GSTM1 and Y10b—Changes in immunolabeling with anti-GSTM1 and the ribosomal antibody, Y10b were directly compared using double-label immunohistochemistry. Cochlea removal was performed and subjects (n=4) were allowed to survive 12 h following surgery. Free-floating sections were collected in PBS, washed 3× in PBS, blocked with 1% normal horse and goat serum and then incubated overnight in both primary antibodies (GSTM1, 1:800 and Y10b, 1:250). The following day, sections were washed with in PBS then incubated with two secondary antibodies: horse-anti-mouse FITC (1:100) for Y10b (Vector Laboratories) and goat anti-rabbit Cy3 (1:100) (Jackson Immunoresearch Laboratories, West Grove, PA, USA) for GSTM1. After washing 3×10 min in PBS, the sections were mounted on electrostatically charged microscope slides, cover-slipped with VectaShield mounting media (Vector Laboratories) and sealed with commercially available nail polish. To minimize quenching, this procedure was performed under restricted lighting.

Data analysis

For objective analysis of immunolabeling, densitometric measurements of NM neurons were obtained using NIH ImageJ. The staining densities of NM neurons on the intact side of the NM were compared with those on the deafferented side of the brain in the same tissue section. For these analyses, the digital image of the tissue was viewed under a 40× objective and captured using a Spot RT camera system. Light levels and contrast settings remained constant throughout analysis. An advantage of the avian brain stem auditory system is that it allows comparison of the relative levels of labeling between opposite sides of the same brain. At least two to three sections from each of three subjects were measured for each antibody. Sections were randomly selected by designating the first and third section on the slide as those to be used for analysis. Brains were only included if the coronal sections were deemed to be symmetrical, so as to avoid possible confounds related to the anterior-to-posterior location of the cells. Neurons with an observable intact cell membrane were analyzed beginning from the most medial region of NM and proceeding laterally. Approximately, 30–40 cells in NM on each side of the section were measured. To prevent bias, the identities of the intact and deafferented sides of the brain were only revealed after measurements were obtained. All data compilations and analyses were performed using Microsoft Excel and SPSS.

Matched pairs of photomicrographs of the deafferented NM were used for objective analysis of the double-label immunohistochemistry. Photomicrographs of the same field using the two different fluorescent filter cubes were captured and the gray scale image of each was analyzed using NIH ImageJ. Anti-Y10b immunolabeling was determined by a densitometric measurement of 30–40 cells selected from medial to lateral NM on the cochlea removal side of the brain while anti-GSTM1 immunolabeling was determined by a densitometric measure

of the nucleus in those same neurons. The correlations between the cytoplasmic labeling using Y10b and the nuclear labeling using anti-GSTM1 were calculated using Microsoft Excel.

RESULTS

Deafferentation-induced elevation in levels of ROS

Unilateral cochlea removal resulted in a transient rise in levels of ROS in the NM neurons. An example of this effect is shown in Fig. 1. Approximately 6–8 h following cochlea removal, deafferented NM neurons exhibit elevated levels of ROS. Opposite sides of the same tissue section were compared for analysis and these objective analyses of staining density confirmed the visual impressions. A two-way mixed analysis of variance (ANOVA) was performed on the gray scale density measurements using side of the brain as the within-subjects variable and time of survival as the between-subjects variable. This analysis did show a reliable main effect of time [$F(2, 11)= 6.2$, $P<0.05$], but the overall main effect of Side was not statistically reliable [$F(1, 11)=0.19$, $P>0.05$]. Importantly, the Group×Side interaction was statistically significant [$F(2, 11)=9.57$, $P<0.05$]. Post hoc (Studen-Newman-Keuls) pair-wise comparisons revealed reliable ($P<0.05$) differences between the intact and cochlea removal side of the brain at 6–8 h following deafferentation. The between-group differences were further analyzed by transforming gray scale scores to percent difference [(mean cochlea removal − mean intact)/ mean intact × 100]. A one-way ANOVA on these percent difference scores revealed that there was a statistically reliable between-group effect [$F(2, 11)= 4.4$, $P<0.05$]. Post hoc pairwise comparisons (Student-Newman-Keuls) showed that the 6–8 h group differed reliably ($P<0.$ 05) from both 3 and 12 h survival times. These percent differences are illustrated in Fig. 2, in which positive numbers indicate that NM neurons on the cochlea removal were more brightly labeled with fluorescent dye than those on the intact side of the brain.

Deafferentation-induced lipid peroxidation

To determine whether the increase in levels of ROS leads to lipid peroxidation in NM, neurons were immunolabeled with anti-4-HNE. Deafferentation led to an increase in lipid peroxidation 6 h following cochlea removal. An example of this effect can be seen in Fig. 3. Once again, objective analyses of staining density confirmed these visual impressions. A two-way mixed ANOVA was performed on the gray scale density measurements using side of the brain as the within-subjects variable and time of survival as the between-subjects variable. This analysis revealed that the main effect of time was not reliable [$F(3, 11)=0.98$, $P>0.05$], however the overall main effect of Side was statistically reliable [$F(1, 11)= 34.13$, $P<0.01$] and the Group×Side interaction was also statistically significant [$F(3, 11)=4.7$, $P<0.05$]. Post hoc (Student-Newman-Keuls) pair-wise comparisons revealed reliable ($P<0.05$) differences between the intact and the cochlea removal side of the brain only at 6 and 12 h following deafferentation.

To further examine the between-group differences, density measurements were normalized across sections and slices by transforming gray scale scores to percent difference scores [(mean cochlea removal − mean intact)/mean intact × 100]. These percent difference data are summarized in Fig. 4, in which positive numbers indicate that NM neurons on the cochlea removal were more darkly labeled than those on the intact side of the brain. A one-way ANOVA on these percent difference scores revealed that there was a statistically reliable between-group effect [$F(3, 11)= 4.2$, $P<0.05$]. Post hoc pair-wise comparisons (Student-Newman-Keuls) showed that the 1 h group differed reliably ($P<0.$ 05) from both 6 and 12 h survival times, but did not differ from the 24 h survival time.

Deafferentation-induced increase in levels of GSTM1

Cochlea removal results in an upregulation of GSTM1 on the deafferented side of the brain. An analysis of the time course of this change showed increased expression by approximately 6 h following cochlea removal. An example of this effect is shown in Fig. 5.

Objective analyses of staining density confirmed these visual impressions. A two-way mixed ANOVA was performed on the gray scale density measurements using side of the brain as the within-subjects variable and survival time as the between-subjects variable. This analysis revealed main effect of time was not reliable [$F(3, 9)=1.1$, $P>0.05$]. The main effect of Side was statistically reliable [$F(1, 9)=19.03$, $P=0.02$] and the Group×Side interaction was also statistically significant [$F(3, 9)=6.7$, $P<0.01$]. Post hoc (Studen-Newman-Keuls) pair-wise comparisons revealed reliable ($P<0.05$) differences between the intact and cochlea removal side of the brain at 6–24 h following cochlea removal. To further examine the between-group differences, density measurements were normalized across sections and slices by transforming gray scale scores to percent difference scores [(mean cochlea removal − mean intact)/mean intact × 100]. These percent difference data are summarized in Fig. 6, in which positive numbers indicate that NM neurons on the cochlea removal side were more darkly labeled than those on the intact side of the brain. A one-way ANOVA on these percent difference scores revealed that there was a statistically reliable between-group effect [$F(3, 9)=4.5$, $P<0.05$].

Deafferentation-induced increase nuclear GSTM1 immunolabeling

Although there is an overall increase in GSTM1 labeling in deafferented NM neurons, this difference is particularly pronounced in the nucleus of the cell (Fig. 5). A paired sample *t*-test comparing mean GSTM1 nuclear labeling on the intact and deafferented sides of the brain at 6 h following deafferentation confirmed that this difference was statistically reliable ($t(2)=-6.9$, $P<0.05$). To assess whether GSTM1 was more heavily expressed in healthy or dying NM neurons, sections were double labeled with Y10b (a marker for ribosomal integrity) and GSTM1. A correlation analysis was performed with levels of Y10b cytoplasmic labeling and levels of GSTM1 nuclear labeling. This analysis revealed a strong positive correlation ($r=.83$), suggesting that neurons that express greater Y10b immunolabeling are also likely to express darker GSTM1 nuclear labeling. An example of this effect can be seen in Fig. 7.

Deafferentation-induced upregulation of Nrf1

Possible changes in the ROS-sensitive transcriptional factor, Nrf1, were evaluated 6 h following cochlea removal. Nrf1 labeling was greater on the deafferented side of the brain. An example of this effect can be seen in Fig. 8. The mean Nrf1 labeling of NM neurons on each side of the brain was compared using a paired sample *t*-test. This analysis confirmed that the observed difference in Nrf1 labeling was statistically reliable ($t(2)=-6.4$, $P<0.05$).

DISCUSSION

The chick brain stem provides a valuable model to explore a possible novel pathway in which ROS could potentially influence cell survival and death following the loss of afferent input. The primary rationale for pursuing the present study was that previous reports indicate a rapid increase in intracellular calcium (Zirpel et al., 1995) and a dramatic mitochondrial proliferation in NM following deafferentation (Hyde and Durham, 1994). It was then hypothesized that deafferentation will lead to a rise in levels of ROS. While not surprising, it is a rather intriguing phenomenon considering ROS are typically a by-product of increased cellular activity (review, Brookes et al., 2004) whereas the overall activity in NM decreases following deafferentation (Lippe et al., 1980). Similarly, mitochondrial proliferation typically occurs in muscle tissue in response to elevated activity (Moyes et al., 1998), but proliferation occurs in NM neurons following the loss of activity. The literature has very few examples in which the removal of

afferent input produces an increase in levels of ROS (Miller et al., 2002). Therefore, the chick auditory brain stem is unusual in that neurons showed a deafferentation-induced increase in levels of ROS.

A population of neurons in NM dies within a few days following the removal of auditory nerve activity. Studies aimed at elucidating the nature of the activity-dependent trophic influence suggest that activation of metabotropic glutamate receptors (mGluRs) is required to maintain calcium homeostasis (Zirpel and Rubel, 1996; Zirpel et al., 1998, 2000) and ribosomal integrity (Hyson, 1998; Nicholas and Hyson, 2004) in NM neurons. Still unknown, however, is the precise sequence of events that leads toward cell death following the loss of mGluR activation. Additionally, it is not known what determines whether or not an individual NM neuron will die. Only 20–30% of the neurons die following deafferentation despite the fact that all of the neurons are completely deprived of auditory nerve input. The results from the present set of experiments suggest that oxidative stress and compensatory responses to this stress may play a role in controlling cell death following deafferentation.

It is possible that an early increase in calcium initiates a secondary rise in levels of ROS (Kruman et al., 1998; review, Waring, 2005). In the present study, deafferented NM neurons exhibited elevated levels of ROS by 6 h following cochlea removal. Interestingly, this early rise coincides with mitochondrial proliferation (Hyde and Durham, 1994) and the separation of NM neurons into living and dying populations based on analyses of ribosomal structure and function (Steward and Rubel, 1985; Garden et al., 1994). While suggestive of a causal role, it must be acknowledged that it is not known if the rise in ROS initiates a cascade of events culminating in cell death, or if the rise is simply an indicator of compromised cellular activity. The compromised NM neurons, however, are still capable of producing compensatory changes that may offset the possibility of oxidative damage. GSTM1 enzymes were robustly upregulated in both the cytoplasm and the nucleus of NM neurons between 6 and 12 h following deafferentation. To determine if this compensatory response might be related to which neurons survive following deafferentation, NM neurons were double-labeled with Y10b and GSTM1. Y10b labels ribosomal RNA, and the level of Y10b labeling is related to ribosomal dissociation (Garden et al., 1994), which is believed to be an early indicator of cell death (Hyson, 1995, 1998; Nicholas and Hyson, 2004). The strong correlation between Y10b and GSTM1 immunolabeling suggests that GSTM1 expression is upregulated to a greater extent in surviving neurons than in those neurons that are destined to die. The rise in GSTM1 may be induced by the ROS-sensitive transcriptional factor, Nrf1, which is also upregulated during this time.

Calcium and ROS

Converging evidence suggests that loss of calcium homeostasis is the critical factor that leads to the increase in levels of ROS in NM. This assertion is supported by studies that show cytoplasmic calcium overload results in non-specific permeabilization of the mitochondrial inner membrane which consequently leads to the elevation in ROS (Brookes, 2005). In the chick brain stem, intracellular calcium is elevated within an hour of deafferentation (Zirpel et al., 1995) whereas in the present study, ROS increase occurs 6 h following deafferentation. This sequence of changes suggests, as is the case in other systems, the early calcium rise could be the initiator of the subsequent increase in levels of ROS in NM.

GST is neuroprotective

It is possible that the protection afforded by GST enzymes may be the critical factor that determines whether a given NM neuron will survive or die following deafferentation. The primary function of GST is to detoxify cells through a GSH conjugation of altered cellular products (Kodym et al., 1999; Cumming et al., 2001). Between 6–12 h following deafferentation, there is a robust upregulation of GSTM1 enzymes, not only in the cytoplasm,

but particularly in the nucleus of NM neurons. Further probing with a double labeling assay for both Y10b, a marker of neuronal viability, and GSTM1 antibodies revealed a strong positive correlation between levels of Y10b and GSTM1 immunolabeling in that darker labeled Y10b neurons also expressed darker GSTM1 nuclear immunolabeling. These results suggest that the 70% of NM neurons that eventually survive deafferentation may possess a greater capacity to combat elevated levels of ROS.

Although not heavily explored in neurons, GSTs' possible protective effect in NM is consistent in several reported studies. For instance, elevated levels of GST have been shown to be associated with increased resistance to apoptosis initiated by a variety of stimuli in lymphoma and hematopoietic cells (Kodym et al., 1999; Cumming et al., 2001). Cytosolic GSH transferases, other protective enzymes, and GSH synthesis (Venugopal and Jaiswal, 1996; Hayes and McMahon, 2001) are upregulated by electrophiles through the Nrf1. The present study also documents a possible relationship between the upregulation of Nrf1 and a corresponding rise in nuclear GSTM1. It remains possible that Nrf2, a potentially more potent activator of antioxidant response element gene expression (Jaiswal, 2004) is also involved. Unfortunately, preliminary data (not shown) revealed that the existing antibodies resulted in highly variable labeling in our system. Consequently no conclusions can be drawn about the relative contributions of Nrf1 and Nrf2 at the present time.

Compensatory antioxidant activity could be neuroprotective in cases where compromised calcium homeostasis is the initiator of cell death. The cell permeant antioxidant MnTBAP reduced cell death induced by the calcium ionophore, A23187, in cultures and embryonic striatal neurons (Petersen et al., 2000). The contribution of other GST enzymes such as GSTO1 to calcium signaling is documented. For instance, GSTO1 has been shown to plays a novel role in regulating intracellular calcium, potentially protecting cells containing RyR2 (ryanodine receptor) from radiation damage and apoptosis induced by calcium mobilization from intracellular stores (Dulhunty et al., 2001). Taken together, data suggest that while ROS may not initiate the process, it is central to propagating the calcium-induced cell death. As noted above, a rise in intracellular calcium might be an initiating step in cell death of NM neurons following deafferentation. Consequently the compensatory rise in GST in NM neurons might contribute to the survival of the majority of neurons following deafferentation.

Other mechanisms of GST neuroprotection

While GST typically detoxifies cells by catalyzing GSH conjugation to electrophiles, it should be noted that other pathways of protection have also been observed. For instance, GSTM1 has been shown to inhibit MEKK1 activity induced by UV and H_2O_2 (Ryoo et al., 2004). The overexpression of GSTM1 interfered with the induction into an apoptotic pathway in a manner independent of GSH catalytic activity. In addition, GSTM1 functions as an endogenous inhibitor of ASK1, a MAP3K of the JNK/SAPK and p38 mitogen-activated protein kinase pathway, thereby suppressing ASK1-mediated cell death (Cho et al., 2001).

Although the present study implicates a possible role for GSTM1 in NM neurons, it should not be assumed that this is the only GST enzyme that contributes to the neuroprotection in NM or that GSTM1 is the primary catalyst in NM. For example, GSTP has also been shown to regulate toxicity in cells (Cumming et al., 2001). The multitude of ROS detoxification pathways underscores the critical role oxidative stress plays in normal cellular functioning. GSTs do not singly detoxify cells, but rather, are a part of an orchestrated pathway. Its effectiveness depends on the combined action of other major players such as glutamate cysteine ligase and GSH synthase to supply GSH, and the action of transporters to remove the GSH conjugates from the cell.

The GSH system is only one possible protective mechanism that may be activated following deafferentation. Activation of Nrf1 may induce expression of other cytoprotective enzymes, such as heme oxygenase (Hertel et al., 2002). The present study did not explore these possible neuroprotective molecules, but the evidence that molecules such as Nrf1 and GST expression increase following deafferentation suggests that a full understanding of cell death in this system will require a more thorough investigation of these detoxifying pathways.

MGluRs

The transneuronal activation of mGluRs appears to be a central factor that regulates viability in NM neurons (Hyson, 1998; Zirpel and Rubel, 1996; Nicholas and Hyson, 2004). These receptors are G-protein-coupled receptors that are divided into three groups based on sequence homology, pharmacology and intracellular signaling pathways. Group I is known to stimulate phosphatidyl inositol hydrolysis whereas group II and III are negatively coupled to cyclic AMP production (Conn and Pin, 1997). In the chick auditory brain stem, group I mGluRs' role in regulating neuronal viability is generally appreciated. For instance, the activation of group I mGluRs has been shown to be necessary for the maintenance of ribosomal integrity, as assessed by Y10b immunolabeling (Nicholas and Hyson, 2004). These receptors are also necessary for maintaining calcium homeostasis in NM (Zirpel and Rubel, 1996). The group I regulated second messenger, protein kinase c (PKC) has been shown to influence calcium levels in NM neurons (Zirpel et al., 1998). In principle, PKC could also be a regulator of levels in ROS. This assertion is supported by previous studies that have shown the loss of PKC activity leads to cell death in neurons exposed to oxidative stress whereas the maintenance of PKC activity protects nerve cells from oxidative stress-induced cell death (Maher, 2001). Additionally, PKC has been reported to phosphorylate Nrf2, which then translocates to the nucleus to activate antioxidant response element gene expression (Jaiswal, 2004). Together these results suggest that PKC could be an important mediator of the protective role of mGluR activation and that part of this role is the protection against the rise in levels of ROS observed in NM.

Acknowledgements

This work was supported by NIH grant DC00858.

References

Andersen JK. Oxidative stress in neurodegeneration: cause or consequence? Nat Med 2004;10:S18–S25. [PubMed: 15298006]

Awasthi YC, Sharma R, Cheng JZ, Yang Y, Sharma A, Singhal SS, Awasthi S. Role of 4-hydroxynonenal in stress-mediated apoptosis signaling. Mol Aspects Med 2003;24:219–230. [PubMed: 12893000]

Born DE, Rubel EW. Afferent influences on brainstem auditory nuclei of the chicken: neurons number and size following cochlea removal. J Comp Neurol 1985;231:435–445. [PubMed: 3968247]

Brookes PS. Mitochondrial H(+) leak and ROS generation: an odd couple. Free Radic Biol Med 2005;38:12–23. [PubMed: 15589367]

Brookes PS, Yoon Y, Robotham JL, Anders MW, Sheu SS. Calcium, ATP, and ROS: a mitochondrial love-hate triangle. Am J Physiol Cell Physiol 2004;287:C817–C833. [PubMed: 15355853]

Cheng JZ, Singhal SS, Saini M, Singhal J, Piper JT, Van Kuijk FJ, Zimniak P, Awasthi YC, Awasthi S. Effects of mGST A4 transfection on 4-hydroxynonenal-mediated apoptosis and differentiation of K562 human erythroleukemia cells. Arch Biochem Biophys 1999;372:29–36. [PubMed: 10562413]

Cheng JZ, Yang Y, Singh SP, Singhal SS, Awasthi S, Pan SS, Singh SV, Zimniak P, Awasthi YC. Two distinct 4-hydroxynonenal metabolizing glutathione S-transferase isozymes are differentially expressed in human tissues. Biochem Biophys Res Commun 2001;282:1268–1274. [PubMed: 11302754]

Cho SG, Lee YH, Park HS, Ryoo K, Kang KW, Park J, Eom SJ, Kim MJ, Chang TS, Choi SY, Shim J, Kim Y, Dong MS, Lee MJ, Kim SG, Ichijo H, Choi EJ. Glutathione S-transferase mu modulates the

stress-activated signals by suppressing apoptosis signal-regulating kinase 1. J Biol Chem 2001;276:12749–12755. [PubMed: 11278289]

Clark AG. The comparative enzymology of the glutathione S-transferases from non-vertebrate organisms. Comp Biochem Physiol B 1989;92:419–446. [PubMed: 2650986]

Conn PJ, Pin JP. Pharmacology and function of metabotropic glutamate receptors. Annu Rev Pharmacol Toxicol 1997;37:205–237. [PubMed: 9131252]

Cui K, Luo X, Xu K, Ven Murthy MR. Role of oxidative stress in neurodegeneration: recent developments in assay methods for oxidative stress and nutraceutical antioxidants. Prog Neuropsychopharmacol Biol Psychiatry 2004;28:771–799. [PubMed: 15363603]

Cumming RC, Lightfoot J, Beard K, Youssoufian H, O'Brien PJ, Buchwald M. Fanconi anemia group C protein prevents apoptosis in hematopoietic cells through redox regulation of GSTP1. Nat Med 2001;7:814–820. [PubMed: 11433346]

Dulhunty A, Gage P, Curtis S, Chelvanayagam G, Board P. The glutathione transferase structural family includes a nuclear chloride channel and a ryanodine receptor calcium release channel modulator. J Biol Chem 2001;276:3319–3323. [PubMed: 11035031]

Durham D, Rubel EW. Afferent influences on brain stem auditory nuclei of the chicken: changes in succinate dehydrogenase activity following cochlea removal. J Comp Neurol 1985;231:446–456. [PubMed: 3968248]

Forman HJ, Dickinson DA, Iles KE. HNE: signaling pathways leading to its elimination. Mol Aspects Med 2003;24:189–194. [PubMed: 12892996]

Garden GA, Canady KS, Lurie DI, Bothwell M, Rubel EW. A biphasic change in ribosomal conformation during transneuronal degeneration is altered by inhibition of mitochondrial, but not cytoplasmic protein synthesis. J Neurosci 1994;14:1994–2008. [PubMed: 8158254]

Hayes JD, Flanagan JU, Jowsey IR. Glutathione transferases. Annu Rev Pharmacol Toxicol 2005;45:51–88. [PubMed: 15822171]

Hayes JD, McMahon M. Molecular basis for the contribution of the antioxidant responsive element to cancer chemoprevention. Cancer Lett 2001;174:103–113. [PubMed: 11689285]

Hertel M, Braun S, Durka S, Alzheimer C, Werner S. Upregulation and activation of the Nrf-1 transcription factor in the lesioned hippocampus. Eur J Neurosci 2002;15:1707–1711. [PubMed: 12059978]

Hyde GE, Durham D. Cytochrome oxidase response to cochlea removal in chicken auditory brainstem neurons. J Comp Neurol 1990;297:329–339. [PubMed: 2168902]

Hyde GE, Durham D. Rapid increase in mitochondrial volume in nucleus magnocellularis neurons following cochlea removal. J Comp Neurol 1994;339:27–48. [PubMed: 8106659]

Hyson RL. Activation of metabotropic glutamate is necessary for transneuronal regulation of ribosomes in chick auditory neurons. Brain Res 1998;809:214–220. [PubMed: 9853113]

Hyson RL. Activity-dependent regulation of ribosomes RNA epitope in the chick cochlear nucleus. Brain Res 1995;672:196–204. [PubMed: 7538417]

Hyson RL, Rubel EW. Activity-dependent regulation of protein synthesis in the brain stem auditory system of the chick requires synaptic activation. J Neurosci 1989;9:2835–2845. [PubMed: 2769367]

Jaiswal AK. Nrf2 signaling in coordinated activation of antioxidant gene expression. Free Radic Biol Med 2004;36:1199–1207. [PubMed: 15110384]

Kang MI, Kobayashi A, Wakabayashi N, Kim SG, Yamamoto M. Scaffolding of Keap1 to the actin cytoskeleton controls the function of Nrf2 as key regulator of cytoprotective phase 2 genes. Proc Natl Acad Sci U S A 2004;101:2046–2051. [PubMed: 14764898]

Kelada SN, Stapleton PL, Farin FM, Bammler TK, Eaton DL, Smith-Weller T, Franklin GM, Swanson PD, Longstreth WT Jr, Checkoway H. Glutathione S-transferase M1, T1, and P1 polymorphisms and Parkinson's disease. Neurosci Lett 2003;337:5–8. [PubMed: 12524158]

Kodym R, Calkins P, Story M. The cloning and characterization of a new stress response protein. A mammalian member of a family of theta class glutathione s-transferase-like proteins. J Biol Chem 1999;8:5131–5137. [PubMed: 9988762]

Kruman I, Guo Q, Mattson MP. Calcium and reactive oxygen species mediate staurosporine-induced mitochondrial dysfunction and apoptosis in PC12 cells. J Neurosci Res 1998;51:293–308. [PubMed: 9486765]

Leung L, Kwong M, Hou S, Lee C, Chan JY. Deficiency of the Nrf1 and Nrf2 transcription factors results in early embryonic lethality and severe oxidative stress. J Biol Chem 2003;278:48021–48029. [PubMed: 12968018]

Lippe WR, Steward O, Rubel EW. The effect of unilateral basilar papilla removal upon nuclei laminaris and magnocellularis of the chick examined with [3H]2-deoxy-D-glucose autoradiography. Brain Res 1980;196:43–58. [PubMed: 7397530]

Liu RM, Gao L, Choi J, Forman HJ. Gamma-glutamylcysteine synthetase: mRNA stabilization and independent subunit transcription by 4-hydroxy-2-nonenal. Am J Physiol 1998;275:L861–L869. [PubMed: 9815102]

Maher P. How protein kinase C activation protects nerve cells from oxidative stress-induced cell death. J Neurosci 2001;21:2929–2938. [PubMed: 11312276]

Miller JM, Miller AL, Yamagata T, Bredberg G, Altschuler RA. Protection and regrowth of the auditory nerve after deafness: neurotrophins, antioxidants and depolarization are effective in vivo. Audiol Neurootol 2002;7:175–179. [PubMed: 12053141]

Moyes CD, Battersby BJ, Leary SC. Regulation of muscle mitochondrial design. J Exp Biol 1998;201:299–307.

Nicholas AH, Hyson RL. Group I and II metabotropic glutamate receptors are necessary for the activity-dependent regulation of ribosomes in chick auditory neurons. Brain Res 2004;1014:110–119. [PubMed: 15212997]

Ohinata Y, Miller JM, Altschuler RA, Schacht J. Intense noise induces formation of vasoactive lipid peroxidation products in the cochlea. Brain Res 2000;878:163–173. [PubMed: 10996147]

Petersen A, Castilho RF, Hansson O, Wieloch T, Brundin P. Oxidative stress, mitochondrial permeability transition and activation of caspases in calcium ionophore A23187-induced death of cultured striatal neurons. Brain Res 2000;857:20–29. [PubMed: 10700549]

Rouimi P, Anglade P, Debrauwer L, Tulliez J. Characterization of pig liver glutathione S-transferases using HPLC-electrospray-ionization mass spectrometry. Biochem J 1996;317:879–884. [PubMed: 8760377]

Rubel EW, Hyson RL, Durham D. Afferent regulation of neurons in the brain stem auditory system. J Neurobiol 1990;21:169–196. [PubMed: 2181062]

Ryoo K, Huh SH, Lee YH, Yoon KW, Cho SG, Choi EJ. Negative regulation of MEKK1-induced signaling by glutathione S-transferase mu. J Biol Chem 2004;279:43589–43594. [PubMed: 15299005]

Steward O, Rubel EW. Afferent influences on brainstem auditory nuclei of the chicken: cessation of amino acid incorporation as an antecedent to age-dependent transneuronal degeneration. J Comp Neurol 1985;231:385–395. [PubMed: 3968244]

Tjalkens RB, Valerio LG Jr, Awasthi YC, Petersen DR. Association of glutathione S-transferase isozyme-specific induction and lipid peroxidation in two inbred strains of mice subjected to chronic dietary iron overload. Toxicol Appl Pharmacol 1998;151:174–181. [PubMed: 9705901]

Venugopal R, Jaiswal AK. Nrf1 and Nrf2 positively and c-Fos and Fra1 negatively regulate the human antioxidant response element-mediated expression of NAD(P)H: quinone oxidoreductase1 gene. Proc Natl Acad Sci U S A 1996;93:14960–14965. [PubMed: 8962164]

Waring P. Redox active calcium ion channels and cell death. Arch Biochem Biophys 2005;434:33–42. [PubMed: 15629106]

Yang Y, Sharma R, Sharma A, Awasthi S, Awasthi YC. Lipid peroxidation and cell cycle signaling: 4-hydroxynonenal, a key molecule in stress mediated signaling. Acta Biochim Pol 2003;50:319–336. [PubMed: 12833161]

Zirpel L, Janowiak MA, Taylor DA, Parks TN. Developmental changes in metabotropic glutamate receptor-mediated calcium homeostasis. Comp Neurol 2000;22:95–106.

Zirpel L, Lachica EA, Lippe WR. Deafferentation increases the intracellular calcium of cochlear nucleus neurons in the embryonic chick. J Neurophysiol 1995;74:1355–1357. [PubMed: 7500157]

Zirpel L, Lippe WR, Rubel EW. Activity-dependent regulation of [Ca2+]i in avian cochlear nucleus neurons: roles of protein kinases A and C and relation to cell death. J Neurophysiol 1998;79:2288 – 2302. [PubMed: 9582205]

Zirpel L, Rubel EW. Eighth nerve activity regulates intracellular calcium concentration of avian cochlear nucleus neurons via a metabotropic glutamate receptor. J Neurophysiol 1996;76:4127–4139. [PubMed: 8985906]

Abbreviations

ACSF
artificial cerebrospinal fluid

ANOVA
analysis of variance

ASK1
apoptosis signal-regulating kinase

BSA
bovine serum albumin

GSH
glutathione

H_2DCFDA
carboxyl-2,7-dichlorodihydrofluorescin diacetate

JNK
jun N-terminal kinase

GSTM1
glutathione-S-transferase M1

GSTs
glutathione-S-transferases

mGluRs
metabotropic glutamate receptors

NM
nucleus magnocellularis

PBS
phosphate-buffered saline

PKC
protein kinase c

ROS
reactive oxygen species

4-HNE
4-hydroxynonenal

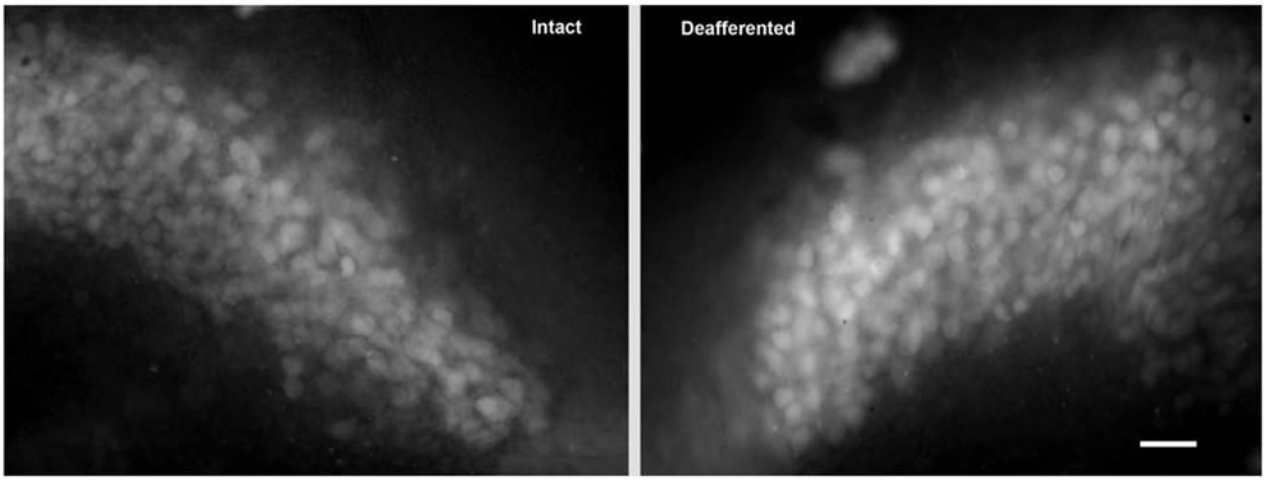

Fig. 1.

Cochlea removal results in a transient rise in levels of ROS in NM neurons. Photomicrograph demonstrating increased levels of ROS, as measured by labeling with H_2DCFDA, 8 h following deafferentation. Opposite sides of the same tissue section were compared for analysis. Scale bar=25 μm.

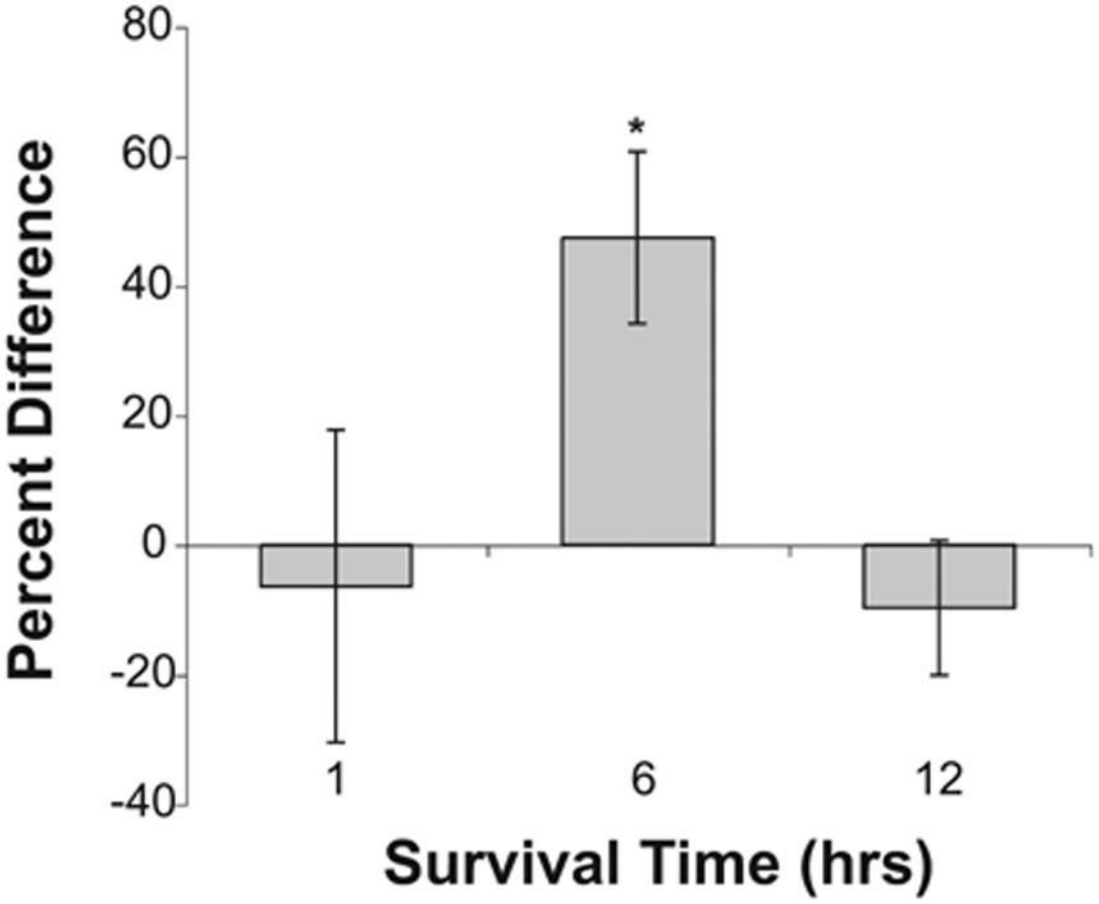

Fig. 2.

Increase in levels of ROS. Percent difference in ROS labeling in NM neurons on opposite sides of the same sections at 1 (*n*=4), 6–8 (*n*=7), or 12 h (*n*=3) following cochlea removal. Positive numbers indicate that the cochlea removal side is more brightly labeled than the intact side of the brain. The asterisk indicates that there is a statistically reliable difference between the deafferented and intact sides of the brain at 6–8 h following deafferentation.

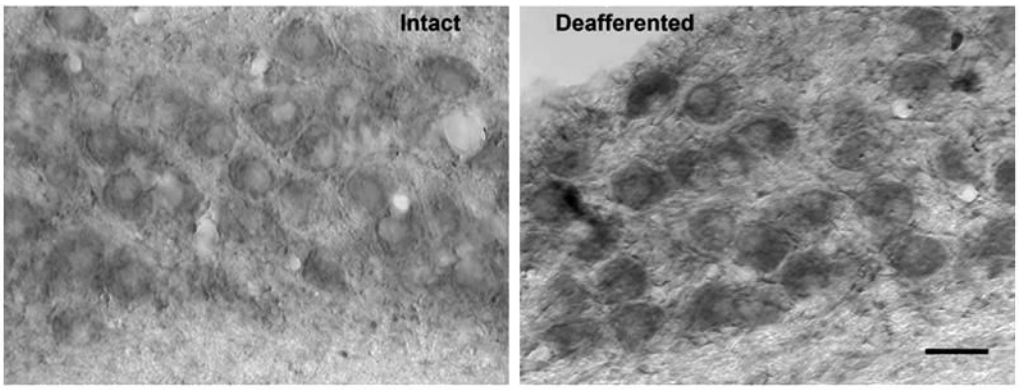

Fig. 3.
Increased lipid peroxidation. Photomicrograph displaying a deafferentation-induced increase in levels of oxidized lipids, as measured by immunolabeling with anti-4-HNE, 6 h following cochlea removal. Opposite sides are compared for analysis. Scale bar=25 μm.

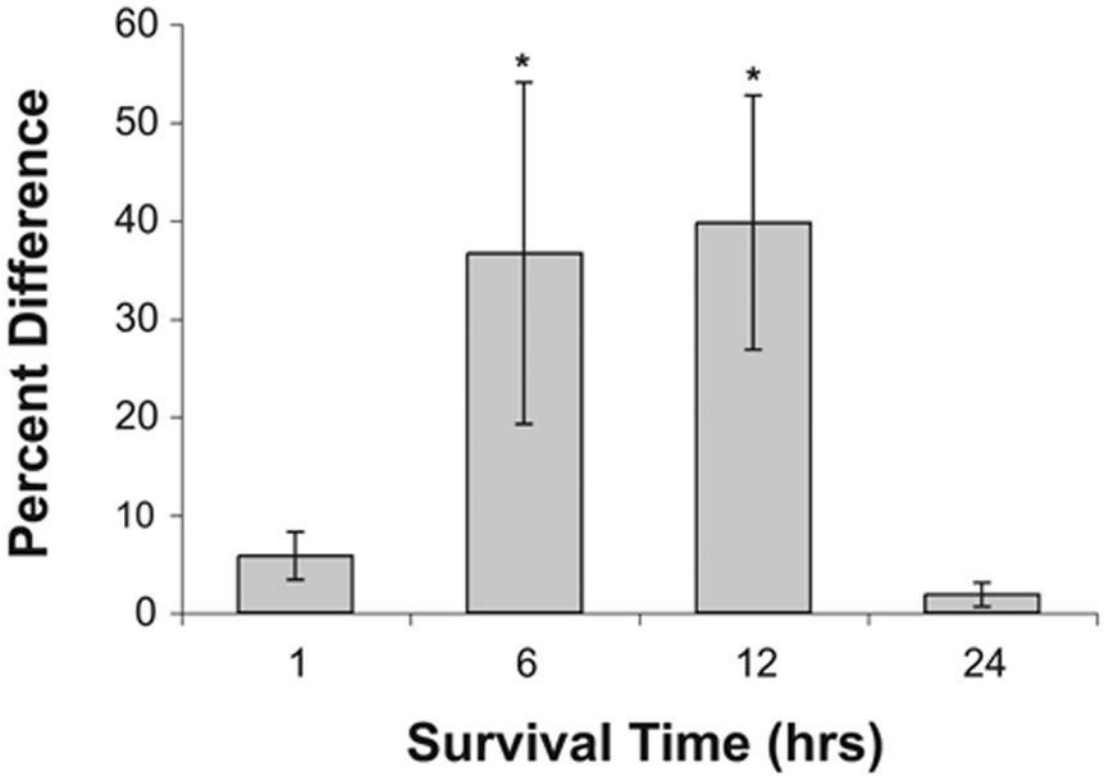

Fig. 4.

Deafferentation-induced lipid peroxidation. Percent difference in immunolabeling in NM neurons on opposite sides of the same section measured 1–3 (*n*=4), 6 (*n*=3), 12 (*n*=5), or 24 h (*n*=3) following deafferentation. Positive numbers indicate that the cochlea removal side is darker than the intact side of the brain. Asterisks indicate that there is a statistically reliable difference between the deafferented and intact sides of the brain. A statistical difference between sides is evident at 6 and 12 h following cochlea removal, but the difference is no longer statistically reliable by 24 h.

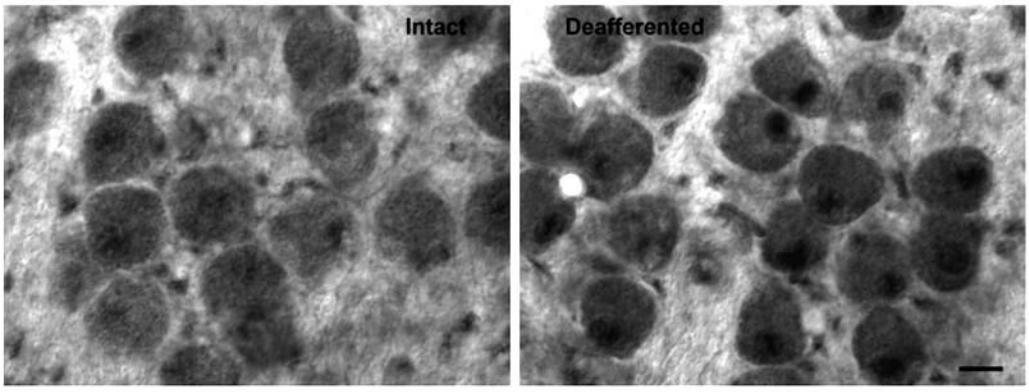

Fig. 5.

Upregulation of GSTM1. Photomicrograph displaying the upregulation of GSTM1 expression in NM neurons 6 h following deafferentation. This suggests that detoxifying compensatory pathways are also increased in response to deafferentation. Note that the difference in the nuclear labeling is particularly pronounced. Opposite sides are compared for analysis. Scale bar=10 μm.

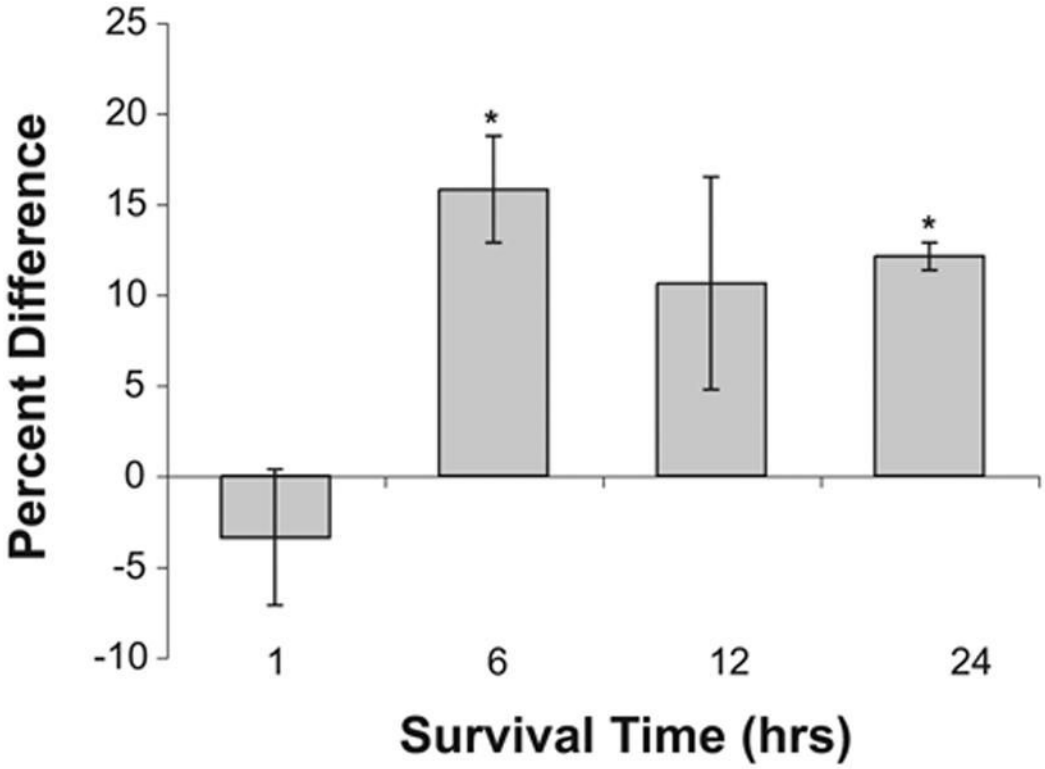

Fig. 6.

Increased GSTM1 expression following deafferentation. Percent difference in immunolabeling in NM neurons on opposite sides of the same sections measured 1 (*n*=3), 6 (*n*=4), 12 (*n*=3), or 24 h (*n*=3) following deafferentation. Positive numbers indicate that the deafferented side is darker than the intact side of the brain. Asterisks indicate that there is a statistically reliable difference between the deafferented and intact sides of the brain.

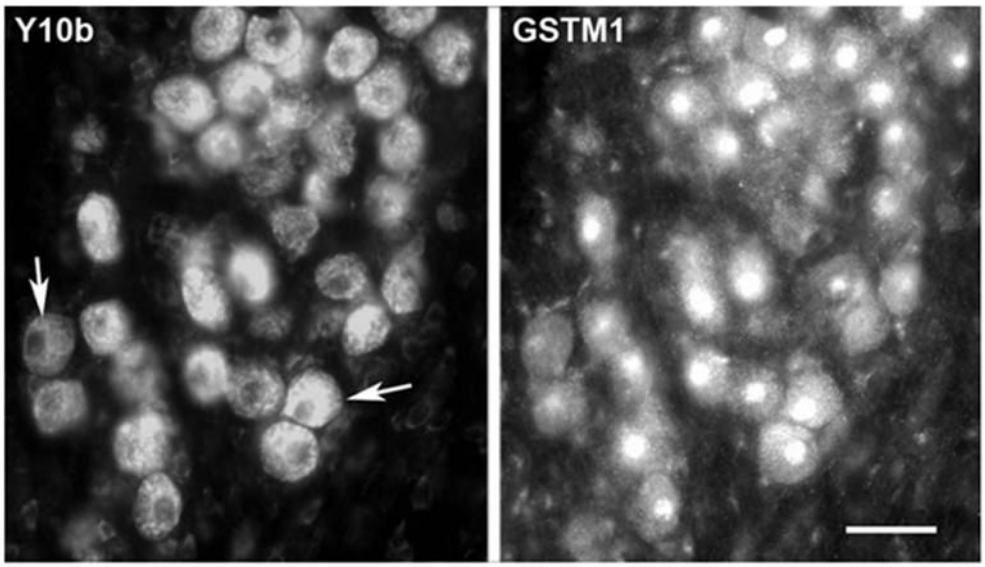

Fig. 7.

Correlated changes in GSTM1 and Y10b immunolabeling. Photomicrographs displaying double-labeling immunofluorescence for Y10b and GSTM1in NM neurons. The left panel displays the labeling with Y10b and the right panel displays the same field showing the GSTM1 immunolabeling. Analysis of labeling in individual cells indicated a positive correlation (r=0.83); neurons that were more darkly labeled with Y10b also express darker GSTM1 nuclear labeling. Arrows point to two examples showing low and high levels of labeling. Scale bar=25 μm.

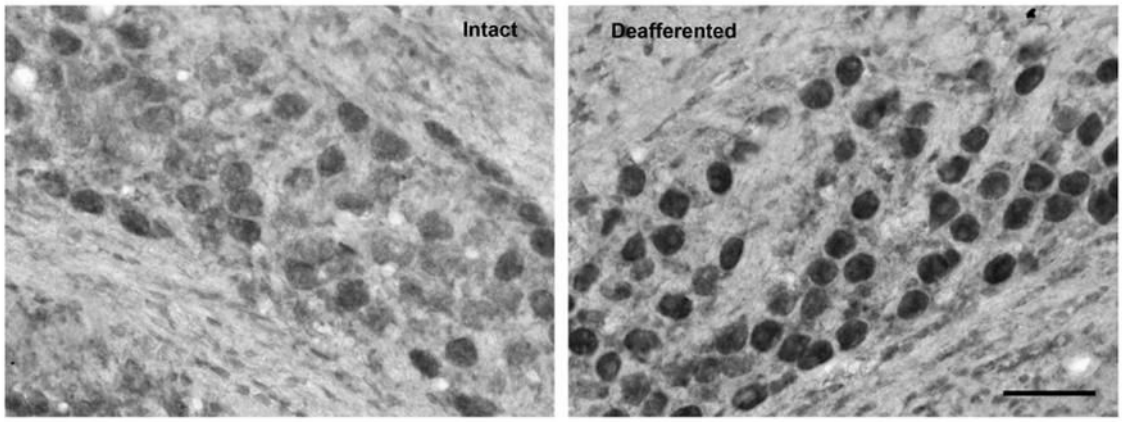

Fig. 8.

Upregulation of Nrf1. Photomicrograph displaying the upregulation of Nrf1expression in NM neurons 6 h following deafferentation. This suggests a possible mechanism for the upregulation of GSTM1. Scale bar=50 μm.